A Self-Cleaning TiO_2 Nanosisal-like Coating toward Disposing Nanobiochips of Cancer Detection

Jingxin Meng,[†] Pengchao Zhang,[‡] Feilong Zhang,[‡] Hongliang Liu,[†] Junbing Fan,[†] Xueli Liu,[‡] Gao Yang,[‡] Lei Jiang,[†] and Shutao Wang*,[†]

[†]Laboratory of Bio-inspired Smart Interface Science, Technical Institute of Physics and Chemistry, Chinese Academy of Sciences, Beijing, 100190, P. R. China, and [‡]Beijing National Laboratory for Molecular Sciences (BNLMS), Key Laboratory of Organic Solids, Institute of Chemistry, Chinese Academy of Sciences, Beijing, 100190, P. R. China

ABSTRACT The advanced nanobiochips have been widely employed in diagnosing some high incidence of diseases because of their portable, low-cost, and highly sensitive features. However, the subsequent disposal of these wastes remains unexposed, probably giving rise to serious environmental pollution and health risks similar to traditional biomedical waste. Here, we have presented a TiO_2 nanosisal-like coating for disposing nanobiochip waste *via* the photoresponsive self-cleaning features of the nanobiochip, demonstrated by the nanochips of cancer detection. Moreover, the high specificity and sensitivity of nanochips can be maintained by integrating unique nanostructured coatings (*i.e.*, nanosisal-like coating) with specific recognition molecules (*i.e.*, anti-EpCAM). Therefore, this study will provide a promising strategy for the design and management of practical nanobiodevices, thereby eliminating the old path "pollute first, clean up later".

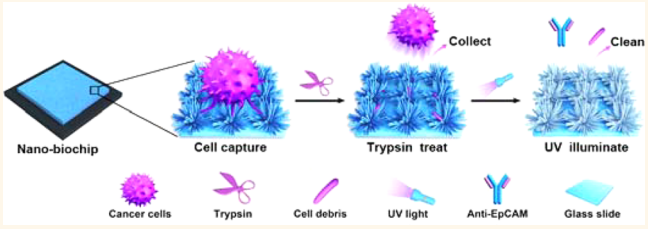

KEYWORDS: nanobiochip · photoresponsive · TiO_2 · self-cleaning · cancer detection

With rapid development of nanobiotechnology and microfabrication technology, nanobiodevices have been widely employed in diagnosing some high incidences of diseases such as hepatitides,[1] Alzheimer,[2,3] and cancers.[4−6] For example, portable and low-cost nanobiochips with high specificity and sensitivity for the detection of disease-related biomarkers including nucleic acid (*e.g.*, DNA or RNA),[7] protein (*e.g.*, peptide),[8−10] and rare cells (*e.g.*, circulating tumor cells, CTCs)[11,12] are gradually growing to the dominated products in current biomedical analysis markets. However, the subsequent disposal of these nanobiochip wastes remains unexposed, probably giving rise to serious environmental pollution and health risks similar to traditional biomedical waste (*e.g.*, syringe needles and catheters).[13] To better circumvent these problems, it is urgent and necessary to develop disposable nanobiochips that can readily manage surface pollutants.

Self-cleaning, as one of the most anticipated and pursued features, attracts great attention because it spends less manpower and resources to manage surface pollutants and thus keep the surface clean.[14−16] Inspired by nature, great effort has been paid to design many promising surfaces with self-cleaning features such as lotus leaf-inspired superhydrophobic surfaces,[17] gecko setae-inspired surfaces,[18] and underwater organisms-inspired antifouling surfaces.[19] However, most of these bioinspired surfaces are still plagued with problems that probably restrict their biomedical applications, especially in the advanced nanobiochips of cancer detection. For example, to endow surfaces with self-cleaning features, it is generally necessary to introduce additional chemical components such as fluorosilane,[20] hydrogel,[21,22] and organogel[23,24] as well as lubricating liquid,[25] which hinder further modification of functional molecules and thus lose the specific recognition capability of targeted cancer cells. In addition, smart-responsive surfaces that respond to external stimuli such as light,[26−28] electricity,[29] magnetism,[30] and temperature,[31,32] are also needed because the persistent self-cleaning feature is not a benefit for the recognition and capture of

* Address correspondence to stwang@mail.ipc.ac.cn.

Received for review July 9, 2015 and accepted August 18, 2015.

Published online August 18, 2015
10.1021/acsnano.5b04230

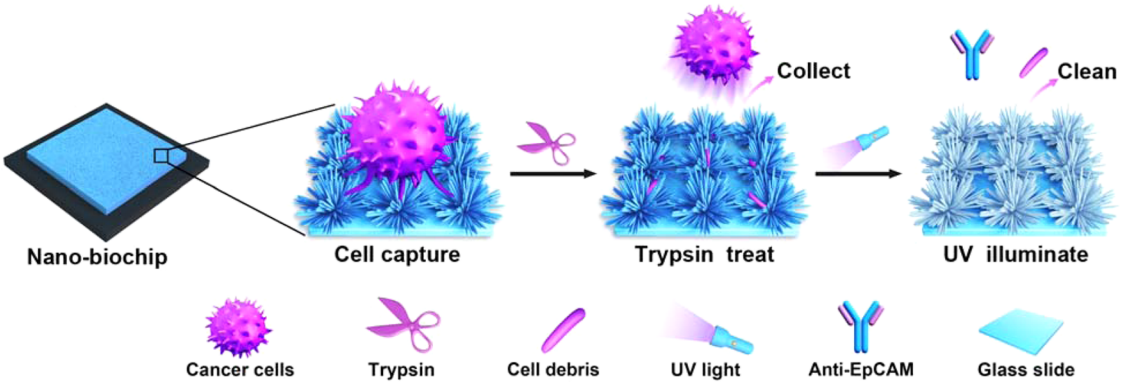

Scheme 1. Schematic illustration of disposing nano-biochips of cancer detection. Firstly, nanobiochips can specifically detect targeted cancer cells by employing the nanosisal-like coating and specific recognition molecule (*i.e.*, anti-EpCAM). Then, captured cells are readily collected for downstream culture and analysis by treating with trypsin because the unique three-dimensional contact mode between captured cells and nano-biochips is a benefit for the entrance of trypsin and subsequent detachment of captured cells. Finally, residual organic pollutants (*e.g.*, cell debris and anti-EpCAM) can be cleaned by utilizing UV illumination

targeted cells.[33] Therefore, smart-responsive self-cleaning surfaces without surface chemical modification may be suitable for fabricating disposable nano-biochips of cancer detection.

Since the first discovery of photoinduced self-cleaning phenomenon of titanium dioxide (TiO_2) by Fujishima and his co-workers, it has been deeply investigated and widely used for self-cleaning surfaces. Different from the above-mentioned self-cleaning surfaces, the self-cleaning features of TiO_2 surfaces are derived from their inherent photoresponsive properties. During the photocatalytic process, the superoxide radicals produced by photo illumination effectively decompose the organic pollutants on the surface of TiO_2 materials into carbon dioxide and water.[34−36] Therefore, TiO_2 materials can be regarded as excellent candidates for preparing disposable devices such as TiO_2 nanotubes for high-sensitivity immunoassay[37] and TiO_2 membranes for selective separation of macromolecules.[38] In addition, water droplets can readily spread over the photoinduced superhydrophilic TiO_2 surfaces, washing away the residual dusts and impurities.[39−42] Thus, these photoresponsive properties endow TiO_2 surfaces with promising self-cleaning features. But how to expand this self-cleaning feature of TiO_2 materials to nanobiochips for the isolation and detection of cancer cells that not only readily remove surface pollutants but also provide satisfying cell-capture performance has not been explored up to now.

In this article, we have developed a TiO_2 nanosisal-like (TiNS) coating for disposing nanobiochip wastes *via* the photoresponsive self-cleaning feature of the nanobiochip, demonstrated by the nanochips for the effecient detection of cancer cells (as shown in Scheme 1). First, targeted cancer cells can be efficiently recognized and captured from artificial whole blood samples *via* the synergistic effect of surface nanosisal-like structures and specific recognition molecules (*i.e.*, epithelial-cell adhesion molecule antibody, anti-EpCAM). Then, captured cancer cells can be readily collected for downstream culture and analysis by treating with trypsin because the unique three-dimensional contact mode between captured cells and nanobiochips is a benefit for the entrance of trypsin and subsequent detachment of captured cells. Significantly, the residual organic pollutants (*e.g.*, cell debris and anti-EpCAM) can be cleaned from the surface of nanobiochips through UV illumination, resulting from the distinguished photodriven self-cleaning features of the TiO_2 coating. Therefore, this study will provide a promising strategy to eliminate serious environmental pollution and health risks caused by nanobiochip waste.

RESULTS AND DISCUSSION

Scanning electron microscopy (SEM) images show that by increasing reaction time of hydrothermal synthesis from 5 and 10 to 20 h, three kinds of nanostructured TiO_2 coatings are precisely prepared with TiNS surface coverage ratios (SCRs) of ca. 24%, 45%, and 100%, denoted as low TiNS (Figure 1a, LTiNS), moderate TiNS (Figure 1b, MTiNS), and high TiNS (Figure 1c, HTiNS), respectively.[43] The X-ray diffraction (XRD) data show that TiNS after calcination is better crystallized in the rutile phase compared with that before calcinations (Figure 1d). Furthermore, transmission electron microscopy (TEM) analysis indicates that the nanorods of TiNS after calcination are rutile phase and grow along the [001] direction (Figure 1ef). The distance between adjacent lattice fringes that run parallel to the nanorod wall was about 0.325 nm, which can be assigned as the interplane distance of (110) planes in the rutile phase of TiO_2 (Figure 1f). Furthermore, the distance between the fringes perpendicular to the wall, about 0.296 nm, corresponds to the interplane distance of the (001) planes in the rutile phase of TiO_2. Therefore, both XRD data and TEM images proved that the subsequent calcination processes not only remove adherent organic pollutants from the hydrothermal reaction but also

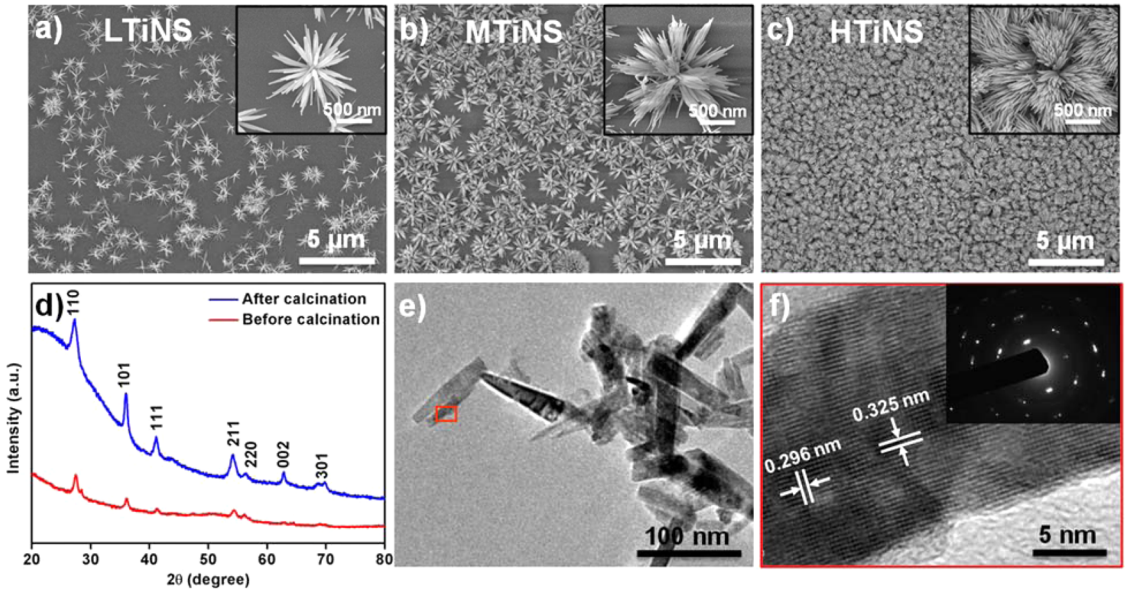

Figure 1. Morphology and characterization of TiNS coating. The SEM images and enlarged SEM images (inset) of three kinds of nanostructured coatings with incremental TiNS SCRs including (a) low TiNS (LTiNS), (b) moderate TiNS (MTiNS), and (c) high TiNS (HTiNS). (d) XRD data of TiNS coatings before and after calcination. (e) Low-magnification TEM image of nanorods on TiNS coatings and (f) the corresponding high-magnification TEM image of an individual nanorod (red rectangle in image e); the inset in image f shows the corresponding selected area electron diffraction (SAED) pattern. Both the XRD data and TEM images show that TiNS coatings are well-crystallized in rutile TiO_2.

endow TiNS coatings (bare TiNS) with better crystallization of TiO_2 rutile phase for promising photocatalytic degradation of organic components.[44−46] Thus, nanobiochips with controllable SCRs of TiNS have been prepared, which may provide distinguished self-cleaning properties toward effectively disposing nanobiochip waste.

To obtain the most appropriate nanobiochips for CTC detection, the influence of two main factors (*i.e.*, cell incubation time and SCRs of TiNS) have been systematically investigated in the following sections. After the modification of anti-EpCAM (see Supporting Information Figure S1),[47] the high specificity of TiNS coating can be confirmed by comparing the capture performance of EpCAM-positive breast cancer cells (*i.e.*, MCF7 cells) using bare, streptavidin-coated, and anti-EpCAM-coated flat and HTiNS coating (Supporting Information Figure S2). To reveal the influence of cell incubation time, we compare cell-capture performance of EpCAM-positive MCF7 cells and two typical EpCAM-negative cancer cells (*i.e.*, the adherent Hela cervical cancer cell[48] and suspended Jurkat T lymphocyte cell[49]) on anti-EpCAM-modified HTiNS coatings in a static incubation ranging from 5 to 90 min (more details in Materials and Methods). As shown in Figure 2a, the capture efficiency of targeted MCF7 cells initially increases with longer incubation time and achieves the maximum value at 60 min. In contrast, the nontargeted Hela and Jurkat T cells always display negligible nonspecific cell adhesion, regardless of incubition time. To further disclose the influence of SCRs of anti-EpCAM-modified TiNS, we compared cell-capture performances on four kinds of anti-EpCAM-modified TiO_2 coatings including flat, LTiNS, MTiNS, and HTiNS (Figure 2b). Under the optimal incubation time (*i.e.*, 60 min), the capture efficiency of targeted MCF7 cells are 58.5% ± 2.9% for anti-EpCAM-modified HTiNS, which is obviously higher than those of other anti-EpCAM-modified TiO_2 coatings (*i.e.*, 8.1% ± 0.5% for flat, 52.1 ± 1.4% for LTiNS, and 53.8% ± 1.8% for MTiNS). Meanwhile, the captured MCF7 cells are still viable with a high viability ratio of *ca.* 97%, proved by a live/dead staining method (Supporting Information Figure S3).[50] Different from targeted MCF7 cells, the nonspecific cell adhesion of nontargeted Hela and Jurkat T cells can be completely neglected on these anti-EpCAM-modified coatings (Figure 2b). Compared with that of anti-EpCAM-modified flat surface, the notable enhancement of cell-capture yield of anti-EpCAM-modified TiNS (*e.g.*, HTiNS) coatings can be explained by notable differences of captured cells in morphology. The environmental SEM (ESEM) images show that the captured cells on the anti-EpCAM-modified HTiNS coating (Figure 2c) not only hold more spreading area but also stretch out more filopodia than those on the anti-EpCAM-modified flat surface (Figure 2d), disclosing an enhanced topographic interaction between targeted cells and HTiNS coating.[51] Therefore, high specificity and sensitivity of CTC detection can be achieved from optimal nanobiochips under 60 min incubation time and HTiNS coatings, resulting from an enhanced topographic interaction between targeted cells and TiNS coating in addition to specific molecular recognition.

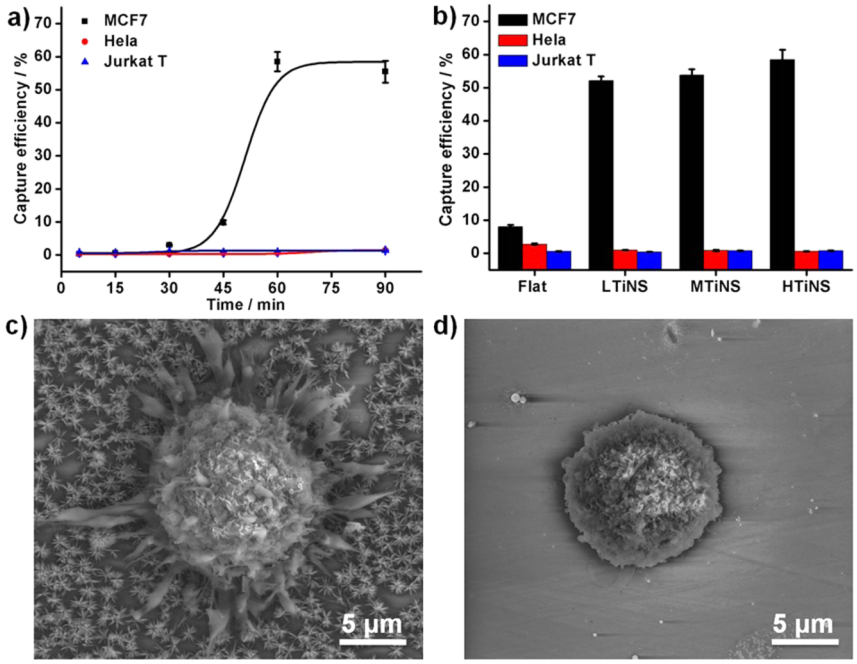

Figure 2. Cell-capture performance of EpCAM-positive MCF7 cells and EpCAM-negative Hela and Jurkat T cells on anti-EpCAM-modified TiO_2 coatings (a) at different incubation times ranging from 5 to 90 min and (b) with four kinds of anti-EpCAM-modified TiO_2 coatings including flat, LTiNS, MTiNS, and HTiNS. Typical ESEM images of MCF7 cells captured on (c) HTiNS and (d) flat surface, respectively. The cells captured by the HTiNS coating exhibited more filopodia than those on the flat surface, indicating the enhanced topographic interaction between targeted MCF7 cells and the HTiNS coating. Error bars: the standard error of mean (n = 3).

To demonstrate the potential clinical application, the capture capability of spiked CTCs from artificial whole blood was tested under the optimized cell-capture conditions (i.e., 60 min incubation time and HTiNS coating). Briefly, we prepared the artificial whole blood samples by spiking healthy mouse blood with DiD-prestained MCF7 cells at concentrations of approximately 20, 50, 100, and 250 cells mL^{-1}. Figure 3a shows that anti-EpCAM-modified HTiNS coatings provide 45−60% capture efficiency of targeted MCF7 cells. To further distinguish spiked MCF7 cells from white blood cells (WBCs) in a artificial whole blood sample, we employed the three-color immunocytochemistry method based on PE-labeled anti-CK (CK, a protein marker for epithelial cells), FITC-labeled anti-CD45 (CD45, a marker for white blood cells), and DAPI for nuclear staining. As shown in Figure 3b, nonprestained MCF7 cells (CK+/CD45-/DAPI+ and 10 μm < cell sizes < 40 μm) can be identified from WBCs (CK-/CD45+/DAPI+, sizes < 15 μm) and cellular debris. Therefore, these results show the potential biomedical application of TiNS coatings for early diagnosis and monitoring of cancer patients.

After CTC detection, these nanobiochip wastes without biosafety disposal may cause serious environmental pollution and health risks.[13] To avoid this unwanted situation, nanobiochips with disposal capability are urgently needed to satisfy clinical demands. Hence, we developed a TiNS coating-based nanobiochip with disposal features taking advantage of its photoresponsive self-cleaning property.[52] Taking the HTiNS coating as an example, the disposal capability of our nanobiochips was investigated from three aspects: *in situ* immunostaining experiments, X-ray photoelectron spectroscopy (XPS) signals, and reusable cell-capture capability. During *in situ* immunostaining experiments, we clearly observed surface variations of HTiNS coatings in the whole disposal process through schematic, optical, and corresponding fluorescent images (Figure 4a). First, targeted MCF7 cells were specifically captured on anti-EpCAM-coated HTiNS coatings after 60 min of cell incubation (left part in Figure 4a).[53] Then, after treating with trypsin (a commonly used enzyme for digesting cells) for a few minutes at 37 °C, all captured MCF7 cells were rapidly detached from HTiNS coatings because the unique three-dimensional contact mode between cells and HTiNS coatings is beneficial to the entrance of trypsin and thus the release of captured cells.[54] However, there remains a little residual cell debris (emphasized with dotted circles in the middle part in Figure 4a). After UV illumination (*i.e.*, 365 nm and 50 mW/cm^2) for 2 h and subsequent PBS wash for several times, the successful disposal of these wastes was observed by cleaning all cell debris (right part in Figure 4a). To further uncover the disposal process, we also explore the XPS signals of four TiNS (*i.e.*, HTiNS) coatings with different chemical components including bare TiNS, anti-EpCAM-coated TiNS, anti-EpCAM-coated TiNS followed by cell release with trypsin (trypsin-treated TiNS), and anti-EpCAM-coated

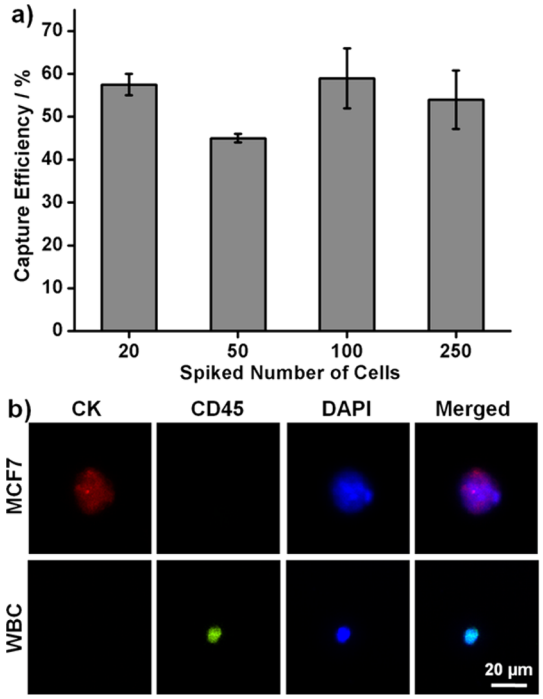

Figure 3. Capture performance of anti-EpCAM-coated TiNS coatings (i.e., HTiNS) for artificial whole blood samples spiked with rare cancer cells (i.e., MCF7). (a) The capture efficiency of prestained MCF7 cells is achieved on anti-EpCAM-coated HTiNS coatings for artificial whole blood samples with concentration of 20, 50, 100, and 250 cells mL^{-1}. (b) Three-color immunocytochemistry method for identifying spiked MCF7 cells from white blood cells (WBCs) including PE-labeled anti-CK (CK, a protein marker for epithelial cells), FITC-labeled anti-CD45 (CD45, a marker for WBCs) and DAPI for nuclear staining. Error bars: the standard error of mean (n = 3).

TiNS followed by cell release and UV illumination (UV-illuminated TiNS). As shown in Figure 4b, we find that both N 1s and C 1s signals of anti-EpCAM-coated and trypsin-treated TiNS have an obvious increase compared to that of bare TiNS, indicating the importation of organic pollutants (*e.g.*, cell debris and/or anti-EpCAM). After UV illumination, the N 1s and C 1s signals of UV-illuminated TiNS decrease to their initial intensity as bare TiNS, indicating the successful disposal of surface organic pollutants. In addition, the disposal process of organic pollutants can be also revealed by the initial decrease and subsequent recovery of Ti 2p3 signals. The successful disposal of waste mainly originates from photocatalytic degradation which is in accordance with previous reports.[37,55,56] Since the nanochip waste had already been disposed, we wondered if the nanochips could be reused for cell-capture. After the remodification with the antibody (*i.e.*, anti-EpCAM), similar cell-capture efficiency (*ca.* 55%) can be obtained in four cycles under optimal conditions (*i.e.*, 60 min incubation time and HTiNS coating), revealing the outstanding reusable capability of the nanochips (Figure 4c). Therefore, this solid evidence from *in situ* immunostaining experiments, XPS signals, and reusable cell-capture capability all prove that nanobiochip wastes with TiNS coatings can be successfully disposed because of their UV-driven self-cleaning capability.

CONCLUSION

In summary, we have successfully developed a photoresponsive TiNS coating for disposing nanobiochip waste. By utilizing the synergistic effect of topological interaction and specific molecular recognition, the TiNS coating can efficiently detect CTCs from artificial whole blood samples with high viability. After detaching the captured cells by simply treating with trypsin, the residual organic components on the nanobiochips can be completely disposed through UV illumination, resulting from the self-cleaning features of TiO_2 materials. This study will provide a promising guidance for developing the next-generation of disposable nanobiochips, thereby eliminating the old path "pollute first, clean up later".

MATERIALS AND METHODS

Materials. Titanium isopropoxide (TTIP, 98%) was purchased from J&K Scientific, cetyltrimethylammonium bromide (CTAB, 99%) was purchased from Acros Organics, ethylene glycol (EG) was purchased from Xilong Chemical Co. Ltd., doubly distilled water (>1.82 MΩ cm, Milli-Q system) was used. Sulfuric acid (95%−98%, AR), hydrogen peroxide (30%, AR), acetone (>99.5%, AR), alcohol (≥99.8%, GR), hydrochloric acid (36%−38%, AR) and dimethyl sulfoxide (99.5%, AR) were purchased from Beijing Chemical Works. Urea, 4-maleimidobutyric acid *N*-hydroxysuccinimide ester (GMBS) and 3-mercaptopropyl trimethoxysilane (95%, MPTMS) were purchased from Sigma-Aldrich Co. Streptavidin (SA) and biotinylated antihuman EpCAM antibody (biotinylated anti-EpCAM) were obtained from R&D systems. Lymphocyte cell line (Jurkat T), cervical cancer cell line (Hela), and breast cancer cell line (MCF7) were purchased from Beijing Xiehe Cell Resource Center. Triton X-100 was purchased from Amresco. Paraformaldehyde (AR) was purchased from Aladdin. DiD, DAPI, AO, and PI were purchased from BioDev-Tech Co. China. Primary antibody (antivinculine mouse monoclonal), secondary antibody (FITC-conjugated goat antimouse), and TRITC-conjugated phalloidin were purchased from Sigma-Aldrich. Penicillin−streptomycin and phosphate buffer solution (PBS) were purchased from Thermo Scientific. GlutaMAX-I, trypsin-EDTA, DMEM, and RPMI-1640 growth medium were obtained from Invitrogen. Fetal bovine serum (FBS) was obtained from Lonza. Male Wistar rats (300−320 g) were purchased from Vital River Laboratory Animal Center (Beijing, China).

Fabrication of the TiO_2 Nanosisal-like (TiNS) Coating. We deposited TiNS coatings on glass slides by the combination of hydrothermal reaction and calcination.[43] First, the glass slides (1 cm × 2 cm) were cleaned according to the following procedure. The glass slides were ultrasonicated in acetone, ethanol, and doubly distilled water at room temperature for 10, 10, and 5 min, respectively, to remove contamination from organic grease. Then, the degreased glass slides were heated in boiling piranha solution (3:1 (v/v) H_2SO_4/H_2O_2) for 1 h. Subsequently, the glass slides were rinsed several times with doubly distilled water and dried by N_2 flow. Then, the clean glass slides were vertically placed in a 45 mL autoclave. In a typical experimental procedures, 0.45 g of TTIP was added into 13.8 g of concentrated HCl

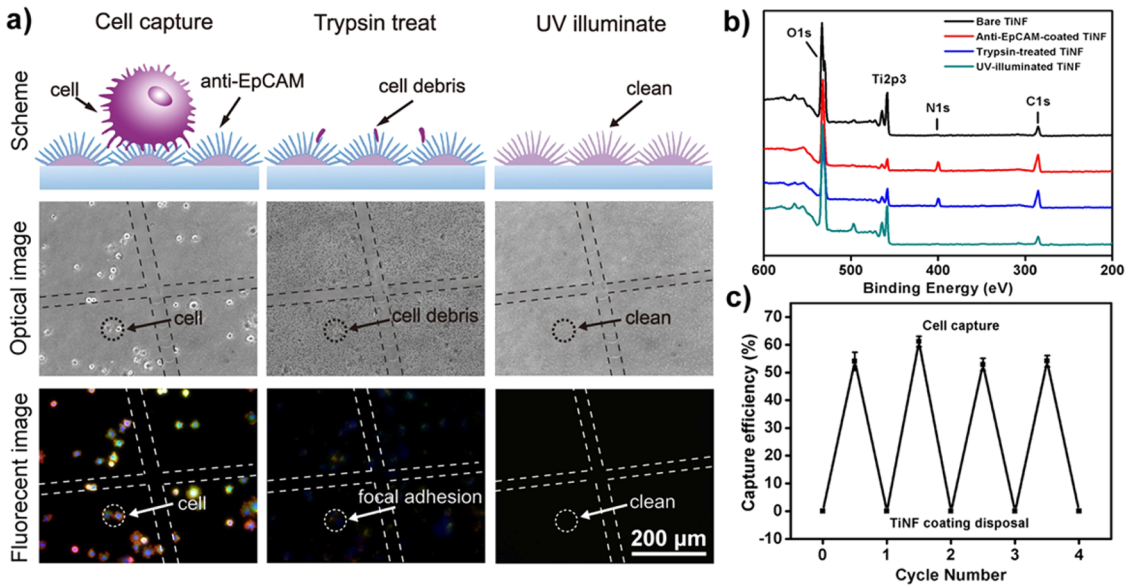

Figure 4. Disposal process of nanobiochips covered by TiNS coating is proven by *in situ* immunostaining experiments, XPS signals, and reusable cell-capture capability. (a) The *in situ* immunostaining experiments revealed the disposal process through schematic (top), optical (middle), and corresponding fluorescent images (bottom). After 60 min of incubation, targeted cancer cells (*i.e.*, MCF7 cells) were captured on anti-EpCAM-coated HTiNS coating (left). After treating with trypsin, the captured cells were completely released with a little cell debris being left (middle). After UV illumination, all cell debris and corresponding focal adhesions were cleaned (right). Dotted lines represent the cross symbol area premarked on the HTiNS coating by a sharp needle before cell-capture for *in situ* observation. Dotted circles are used to emphasize the disposal process of cell debris and corresponding focal adhesions. The captured MCF7 cells were costained for actin (red), vinculin (a universal biomarker of focal adhesion, green), and nuclei (blue) (scale bar: 200 μm). (b) XPS patterns show that C 1s, N 1s, and Ti 2p3 signals return to their initial state after UV illumination, indicating the removal of organic pollutants. (c) After coating anti-EpCAM, the same HTiNS coatings exhibit similar cell-capture performance (*ca.* 55%) in four cycles, demonstrating the reusable capability of TiNS coating.

solution during strong stirring (bottle A), and 0.22 g of CTAB was added into 27.3 mL of distilled water to form aqueous CTAB solution (bottle B). After the mixtures were stirred for 30 min, bottle B was added into bottle A and this mixture was stirred for 1 h to form the aqueous TTIP solution. Then, EG with the same volume was added into the aqueous TTIP solution. After this solution was stirred for 10 min, 0.06 g of urea was added into 25 mL of the mixture of the aqueous TTIP solution and EG. After 10 min of stirring, the formed aqueous solution was transferred to the autoclave containing glass slides. The solution was heated at 150 °C for different times (*i.e.*, 5, 10, and 20 h) and cooled to room temperature. The glass slides coated by TiNS coatings were washed with alcohol three times and allowed to dry at room temperature, followed by heating at 450 °C for 2 h. The TiNS coatings were fabricated showing different coverage ratios from 24% and 45% to 100%.

Surface Modification with anti-EpCAM. We modify anti-EpCAM onto flat TiO_2 and TiNS coatings for specific recognition of targeted cancer cells.[50] Prior to the surface modification, these coatings were first treated with oxygen plasma at 150 w for 300 s (DT-03, China). Then, the TiO_2 coatings were treated with 4% (v/v) 3-mercaptopropyl trimethoxysilane (MPTMS) in ethanol at room temperature for about 12 h. Then, to coat GMBS onto the TiO_2 coatings, these coatings were treated with the coupling agent 4-maleimidobutyric acid *N*-hydroxysuccinimide ester (GMBS, 0.25 mM) for 45 min. Finally, these coatings were treated with 10 μg mL^{-1} of SA at room temperature for 30 min, resulting in immobilization onto GMBS, and then flushed with 1× PBS to remove excess streptavidin. To use for a long-term, all these TiO_2 coatings should be sealed and stored at 4−8 °C. Before cell capture experiments, antibodies (biotinylated anti-EpCAM, 10 μg/mL in PBS) were grafted onto the TiO_2 coatings at room temperature for 30 min for specifically recognizing targeted cancer cells.

Cell-Capture Condition. After placing the anti-EpCAM modified substrates (*e.g.*, HTiNS) into six-well cell culture plates, 3 mL of cell suspensions with a concentration of 10^5 cells/mL was gently added into each well and incubated in a static state in cell incubators (37 °C, 0.5% CO_2) with different incubation time. After gently washing these substrates with PBS for three times, the cells were sequentially fixed using paraformaldehyde solution (4 wt % in PBS), penetrated using Triton-X100 (0.2 wt % in PBS), and dyed using DAPI solution (2 μg/mL in water) for fluorescence imaging and counting.

Cell Capture from Whole Blood Samples. This procedure was depicted in our previous work.[50] DiD-prestained MCF7 cells were first spiked into healthy mouse blood to prepare artificial whole blood samples with concentrations of about 20, 50, 100, and 250 cells mL^{-1}. Then, three anti-EpCAM-coated HTiNS coatings were separately covered by 1 mL of prepared blood samples for 60 min. Later, the HTiNS coatings were gently rinsed with PBS solution for three times and employed for fluorescence imaging. Furthermore, the three-color immunocytochemistry method can be used to identify nonprestained cancer cells from whole blood samples. After 60 min of cell capture, the captured cells were sequentially treated with 4% paraformaldehyde in PBS for 20 min and 20 μL of 0.2% Triton X-100 in PBS for 10 min. Then, the cells were sequentially stained with 20 μL of anti-CD45 stock solution (50 μL of antibody stock solution in 1 mL of PBS) for 30 min, 20 μL of anti-CK stock solution (50 μL of antibody stock solution in 1 mL of PBS) for 30 min, and 20 μL of DAPI solution (2 μg mL^{-1} DAPI in PBS) for 15 min, respectively. Finally, these cells were imaged by using an inverted Nikon Ti-E microscope.

Immunofluorescent Staining of Captured MCF7 Cells. This detailed procedure was described in our previous report.[50] The captured MCF7 cells are first incubated with anti-EpCAM-coated TiNS coatings for 60 min. Then, cultured cells are sequentially treated with 4% paraformaldehyde in PBS for 20 min, 0.2% Triton X-100 in PBS for 5 min, and 1% BSA in PBS for 30 min at room temperature. After that, each TiNS coating is sequentially stained with 100 μL of antivinculin mouse monoclonal (diluted 1:400 in PBS) for 1 h, 100 μL of FITC-conjugated goat antimouse (diluted 1:30 in PBS) for 30 min, and 100 μL of TRITC-conjugated

phalloidin (15 μg in 250 μL methanol and diluted 1:40 in 1% BSA in PBS) for 30 min, as well as 100 μL of DAPI (2 μg/mL) diluted by PBS for 5 min, respectively. Finally, fluorescence images of captured MCF7 cells can be observed and captured with a Nikon Ti-E fluorescence microscope.

The Determination of UV Illumination Conditions. To select the proper UV excitation wavelength, we tested the UV−vis absorption spectrum of TiNS coating by using a UV−vis spectrophotometer (Shimadzu UV2600). Two apparent absorption peaks (*i.e.*, 330 and 400 nm) can be observed in Figure S4. Therefore, the commonly used 365 nm was used as the excitation wavelength. The selected illumination intensity (*i.e.*, 50 mW/cm^2) was determined by the optical power/energy meter (Newport model 842-PE).

Conflict of Interest: The authors declare no competing financial interest.

Supporting Information Available: The Supporting Information is available free of charge on the ACS Publications website at DOI: 10.1021/acsnano.5b04230.

The schematic view of chemical modification process of TiO_2 coatings; the comparison of the capture efficiency of targeted MCF7 cells using bare, streptavidin-coated, and anti-EpCAM-coated flat surface and TiNS coating (*i.e.*, HTiNS); the fluorescent microscope image of MCF7 cells captured on anti-EpCAM-coated HTiNS coating with live/dead staining; the UV−vis absorption spectrum of HTiNS coating (PDF)

Acknowledgment. This research is supported by the National Research Fund for Fundamental Key Projects (2012CB933800), National Natural Science Foundation (21175140, 21425314, 21434009 and 21421061), the Key Research Program of the Chinese Academy of Sciences (KJZD-EW-M01), the National High Technology Research and Development Program of China (863 Program) (2013AA032203), MOST (2013YQ190467).

REFERENCES AND NOTES

1. Bartenschlager, R.; Lohmann, V.; Penin, F. The Molecular and Structural Basis of Advanced Antiviral Therapy for Hepatitis C Virus Infection. *Nat. Rev. Microbiol.* **2013**, *11*, 482–496.
2. Li, M.; Yang, X.; Ren, J.; Qu, K.; Qu, X. Using Graphene Oxide High Near-Infrared Absorbance for Photothermal Treatment of Alzheimer's Disease. *Adv. Mater.* **2012**, *24*, 1722–1728.
3. Geng, J.; Li, M.; Ren, J.; Wang, E.; Qu, X. Polyoxometalates as Inhibitors of the Aggregation of Amyloid β Peptides Associated with Alzheimer's Disease. *Angew. Chem.* **2011**, *123*, 4270–4274.
4. Myung, J. H.; Launiere, C. A.; Eddington, D. T.; Hong, S. Enhanced Tumor Cell Isolation by a Biomimetic Combination of E-selectin and Anti-EpCAM: Implications for the Effective Separation of Circulating Tumor Cells (CTCs). *Langmuir* **2010**, *26*, 8589–8596.
5. Jeon, S. H.; Moon, J. M.; Lee, E. S.; Kim, Y. H.; Cho, Y. An Electroactive Biotin-Doped Polypyrrole Substrate That Immobilizes and Releases EpCAM-Positive Cancer Cells. *Angew. Chem.* **2014**, *126*, 4685–4690.
6. Sheng, W. A.; Chen, T.; Tan, W. H.; Fan, Z. H. Multivalent DNA Nanospheres for Enhanced Capture of Cancer Cells in Microfluidic Devices. *ACS Nano* **2013**, *7*, 7067–7076.
7. Cao, Y. C.; Jin, R.; Mirkin, C. A. Nanoparticles with Raman Spectroscopic Fingerprints for DNA and RNA Detection. *Science* **2002**, *297*, 1536–1540.
8. Zhao, Z.; Zhu, L.; Bu, X.; Ma, H.; Yang, S.; Yang, Y.; Hu, Z. Label-Free Detection of Alzheimer's Disease through the ADP3 Peptoid Recognizing the Serum Amyloid-beta42 Peptide. *Chem. Commun.* **2015**, *51*, 718–721.
9. Wang, X.; Gan, H.; Sun, T. Chiral Design for Polymeric Biointerface: The Influence of Surface Chirality on Protein Adsorption. *Adv. Funct. Mater.* **2011**, *21*, 3276–3281.
10. Qing, G.; Zhao, S.; Xiong, Y.; Lv, Z.; Jiang, F.; Liu, Y.; Chen, H.; Zhang, M.; Sun, T. Chiral Effect at Protein/Graphene Interface: A Bioinspired Perspective To Understand Amyloid Formation. *J. Am. Chem. Soc.* **2014**, *136*, 10736–10742.
11. Yoon, H. J.; Kim, T. H.; Zhang, Z.; Azizi, E.; Pham, T. M.; Paoletti, C.; Lin, J.; Ramnath, N.; Wicha, M. S.; Hayes, D. F.; et al. Sensitive Capture of Circulating Tumour Cells by Functionalized Graphene Oxide Nanosheets. *Nat. Nanotechnol.* **2013**, *8*, 735–741.
12. Wang, S. T.; Liu, K.; Liu, J. A.; Yu, Z. T. F.; Xu, X. W.; Zhao, L. B.; Lee, T.; Lee, E. K.; Reiss, J.; Lee, Y. K.; et al. Highly Efficient Capture of Circulating Tumor Cells by Using Nanostructured Silicon Substrates with Integrated Chaotic Micromixers. *Angew. Chem., Int. Ed.* **2011**, *50*, 3084–3088.
13. Babanyara, Y.; Ibrahim, D.; Garba, T.; Bogoro, A.; Abubakar, M. Poor Medical Waste Management (MWM) Practices and Its Risks to Human Health and the Environment: A Literature Review. *Waste Manage* **2013**, *7*, 512–519.
14. Liu, K.; Jiang, L. Bio-Inspired Self-Cleaning Surfaces. *Annu. Rev. Mater. Res.* **2012**, *42*, 231–263.
15. Ganesh, V. A.; Raut, H. K.; Nair, A. S.; Ramakrishna, S. A Review on Self-Cleaning Coatings. *J. Mater. Chem.* **2011**, *21*, 16304–16322.
16. Liu, K. S.; Yao, X.; Jiang, L. Recent Developments in Bio-inspired Special Wettability. *Chem. Soc. Rev.* **2010**, *39*, 3240–3255.
17. Feng, L.; Li, S.; Li, Y.; Li, H.; Zhang, L.; Zhai, J.; Song, Y.; Liu, B.; Jiang, L.; Zhu, D. Super-Hydrophobic Surfaces: From Natural to Artificial. *Adv. Mater.* **2002**, *14*, 1857–1860.
18. Hansen, W. R.; Autumn, K. Evidence for Self-Cleaning in Gecko Setae. *Proc. Natl. Acad. Sci. U. S. A.* **2005**, *102*, 385–389.
19. Ball, P. Engineering Shark Skin and Other Solutions. *Nature* **1999**, *400*, 507–509.
20. Wang, H.; Xue, Y.; Ding, J.; Feng, L.; Wang, X.; Lin, T. Durable, Self-Healing Superhydrophobic and Superoleophobic Surfaces from Fluorinated-Decyl Polyhedral Oligomeric Silsesquioxane and Hydrolyzed Fluorinated Alkyl Silane. *Angew. Chem., Int. Ed.* **2011**, *50*, 11433–11436.
21. Liu, M.; Wang, S.; Wei, Z.; Song, Y.; Jiang, L. Bioinspired Design of a Superoleophobic and Low Adhesive Water/Solid Interface. *Adv. Mater.* **2009**, *21*, 665–669.
22. Cai, Y.; Lin, L.; Xue, Z.; Liu, M.; Wang, S.; Jiang, L. Filefish-Inspired Surface Design for Anisotropic Underwater Oleophobicity. *Adv. Funct. Mater.* **2014**, *24*, 809–816.
23. Liu, H.; Zhang, P.; Liu, M.; Wang, S.; Jiang, L. Organogel-based Thin Films for Self-Cleaning on Various Surfaces. *Adv. Mater.* **2013**, *25*, 4477–4481.
24. Zhang, P.; Liu, H.; Meng, J.; Yang, G.; Liu, X.; Wang, S.; Jiang, L. Grooved Organogel Surfaces towards Anisotropic Sliding of Water Droplets. *Adv. Mater.* **2014**, *26*, 3131–3135.
25. Wong, T. S.; Kang, S. H.; Tang, S. K. Y.; Smythe, E. J.; Hatton, B. D.; Grinthal, A.; Aizenberg, J. Bioinspired Self-Repairing Slippery Surfaces with Pressure-Stable Omniphobicity. *Nature* **2011**, *477*, 443–447.
26. Shin, D. S.; Hyun Seo, J.; Sutcliffe, J. L.; Revzin, A. Photolabile Micropatterned Surfaces for Cell Capture and Release. *Chem. Commun.* **2011**, *47*, 11942–11944.
27. Li, W.; Wang, J.; Ren, J.; Qu, X. 3D Graphene Oxide-Polymer Hydrogel: Near-Infrared Light-Triggered Active Scaffold for Reversible Cell Capture and On-Demand Release. *Adv. Mater.* **2013**, *25*, 6737–6743.
28. Li, W.; Wang, J.; Ren, J.; Qu, X. Near-Infrared Upconversion Controls Photocaged Cell Adhesion. *J. Am. Chem. Soc.* **2014**, *136*, 2248–2251.
29. Ng, C. C. A.; Magenau, A.; Ngalim, S. H.; Ciampi, S.; Chockalingham, M.; Harper, J. B.; Gaus, K.; Gooding, J. J. Using an Electrical Potential to Reversibly Switch Surfaces between Two States for Dynamically Controlling Cell Adhesion. *Angew. Chem., Int. Ed.* **2012**, *51*, 7706–7710.
30. Yu, X.; He, R.; Li, S.; Cai, B.; Zhao, L.; Liao, L.; Liu, W.; Zeng, Q.; Wang, H.; Guo, S. S.; et al. Magneto-Controllable Capture and Release of Cancer Cells by Using a Micropillar Device Decorated with Graphite Oxide-Coated Magnetic Nanoparticles. *Small* **2013**, *9*, 3895–3901.
31. Kim, Y. J.; Ebara, M.; Aoyagi, T. A Smart Nanofiber Web That Captures and Releases Cells. *Angew. Chem., Int. Ed.* **2012**, *51*, 10537–10541.

32. Gurkan, U. A.; Tasoglu, S.; Akkaynak, D.; Avci, O.; Unluisler, S.; Canikyan, S.; MacCallum, N.; Demirci, U. Smart Interface Materials Integrated with Microfluidics for On-Demand Local Capture and Release of Cells. *Adv. Healthcare Mater.* **2012**, *1*, 661–668.
33. Tamada, Y.; Ikada, Y. Effect of Preadsorbed Proteins on Cell Adhesion to Polymer Surfaces. *J. Colloid Interface Sci.* **1993**, *155*, 334–339.
34. Fujishima, A.; Rao, T. N.; Tryk, D. A. Titanium Dioxide Photocatalysis. *J. Photochem. Photobiol., C* **2000**, *1*, 1–21.
35. Chalasani, R.; Vasudevan, S. Cyclodextrin-Functionalized Fe_3O_4@TiO_2: Reusable, Magnetic Nanoparticles for Photocatalytic Degradation of Endocrine-Disrupting Chemicals in Water Supplies. *ACS Nano* **2013**, *7*, 4093–4104.
36. Chen, C.; Ma, W.; Zhao, J. Semiconductor-Mediated Photodegradation of Pollutants under Visible-Light Irradiation. *Chem. Soc. Rev.* **2010**, *39*, 4206–4219.
37. Song, Y. Y.; Schmidt-Stein, F.; Berger, S.; Schmuki, P. TiO_2 Nano Test Tubes as a Self-Cleaning Platform for High-Sensitivity Immunoassays. *Small* **2010**, *6*, 1180–1184.
38. Roy, P.; Dey, T.; Lee, K.; Kim, D.; Fabry, B.; Schmuki, P. Size-Selective Separation of Macromolecules by Nanochannel Titania Membrane with Self-Cleaning (Declogging) Ability. *J. Am. Chem. Soc.* **2010**, *132*, 7893–7895.
39. Wang, R.; Hashimoto, K.; Fujishima, A.; Chikuni, M.; Kojima, E.; Kitamura, A.; Shimohigoshi, M.; Watanabe, T. Light-Induced Amphiphilic Surfaces. *Nature* **1997**, *388*, 431–432.
40. Feng, X. J.; Zhai, J.; Jiang, L. The Fabrication and Switchable Superhydrophobicity of TiO_2 Nanorod Films. *Angew. Chem., Int. Ed.* **2005**, *44*, 5115–5118.
41. Sun, R.-D.; Nakajima, A.; Fujishima, A.; Watanabe, T.; Hashimoto, K. Photoinduced Surface Wettability Conversion of ZnO and TiO_2 Thin Films. *J. Phys. Chem. B* **2001**, *105*, 1984–1990.
42. Wang, R.; Hashimoto, K.; Fujishima, A.; Chikuni, M.; Kojima, E.; Kitamura, A.; Shimohigoshi, M.; Watanabe, T. Photogeneration of Highly Amphiphilic TiO_2 Surface. *Adv. Mater.* **1998**, *10*, 135–138.
43. Sun, Z.; Kim, J. H.; Zhao, Y.; Bijarbooneh, F.; Malgras, V.; Lee, Y.; Kang, Y. M.; Dou, S. X. Rational Design of 3D Dendritic TiO_2 Nanostructures with Favorable Architectures. *J. Am. Chem. Soc.* **2011**, *133*, 19314–19317.
44. Sun, J.; Gao, L.; Zhang, Q. Synthesizing and Comparing the Photocatalytic Properties of High Surface Area Rutile and Anatase Titania Nanoparticles. *J. Am. Ceram. Soc.* **2003**, *86*, 1677–1682.
45. Murakami, N.; Katayama, S.; Nakamura, M.; Tsubota, T.; Ohno, T. Dependence of Photocatalytic Activity on Aspect Ratio of Shape-Controlled Rutile Titanium(IV) Oxide Nanorods. *J. Phys. Chem. C* **2011**, *115*, 419–424.
46. Bae, E.; Murakami, N.; Ohno, T. Exposed Crystal Surface-Controlled TiO_2 Nanorods Having Rutile Phase from $TiCl_3$ under Hydrothermal Conditions. *J. Mol. Catal. A: Chem.* **2009**, *300*, 72–79.
47. Zhang, N. G.; Deng, Y. L.; Tai, Q. D.; Cheng, B. R.; Zhao, L. B.; Shen, Q. L.; He, R. X.; Hong, L. Y.; Liu, W.; Guo, S. S.; et al. Electrospun TiO_2 Nanofiber-Based Cell Capture Assay for Detecting Circulating Tumor Cells from Colorectal and Gastric Cancer Patients. *Adv. Mater.* **2012**, *24*, 2756–2760.
48. Wang, S. T.; Wang, H.; Jiao, J.; Chen, K. J.; Owens, G. E.; Kamei, K.; Sun, J.; Sherman, D. J.; Behrenbruch, C. P.; Wu, H.; et al. Three-Dimensional Nanostructured Substrates toward Efficient Capture of Circulating Tumor Cells. *Angew. Chem., Int. Ed.* **2009**, *48*, 8970–8973.
49. Liu, X. L.; Chen, L.; Liu, H. L.; Yang, G.; Zhang, P. C.; Han, D.; Wang, S. T.; Jiang, L. Bio-Inspired Soft Polystyrene Nanotube Substrate for Rapid and Highly Efficient Breast Cancer-Cell Capture. *NPG Asia Mater.* **2013**, *5*, e63.
50. Meng, J. X.; Liu, H. L.; Liu, X. L.; Yang, G.; Zhang, P. C.; Wang, S. T.; Jiang, L. Hierarchical Biointerfaces Assembled by Leukocyte-Inspired Particles for Specifically Recognizing Cancer Cells. *Small* **2014**, *10*, 3735–3741.
51. Zhang, P. C.; Chen, L.; Xu, T. L.; Liu, H. L.; Liu, X. L.; Meng, J. X.; Yang, G.; Jiang, L.; Wang, S. T. Programmable Fractal Nanostructured Interfaces for Specific Recognition and Electrochemical Release of Cancer Cells. *Adv. Mater.* **2013**, *25*, 3566–3570.
52. Liu, K. S.; Cao, M. Y.; Fujishima, A.; Jiang, L. Bio-Inspired Titanium Dioxide Materials with Special Wettability and Their Applications. *Chem. Rev.* **2014**, *114*, 10044–10094.
53. Chen, W. Q.; Weng, S. N.; Zhang, F.; Allen, S.; Li, X.; Bao, L. W.; Lam, R. H. W.; Macoska, J. A.; Merajver, S. D.; Fu, J. P. Nanoroughened Surfaces for Efficient Capture of Circulating Tumor Cells without Using Capture Antibodies. *ACS Nano* **2013**, *7*, 566–575.
54. Chen, L.; Liu, X.; Su, B.; Li, J.; Jiang, L.; Han, D.; Wang, S. Aptamer-Mediated Efficient Capture and Release of T Lymphocytes on Nanostructured Surfaces. *Adv. Mater.* **2011**, *23*, 4376–4380.
55. Roy, P.; Berger, S.; Schmuki, P. TiO_2 Nanotubes: Synthesis and Applications. *Angew. Chem., Int. Ed.* **2011**, *50*, 2904–2939.
56. Macak, J. M.; Zlamal, M.; Krysa, J.; Schmuki, P. Self-Organized TiO_2 Nanotube Layers as Highly Efficient Photocatalysts. *Small* **2007**, *3*, 300–304.